Synthesis of coastal subsidence measurements in the Ganges-Brahmaputra Delta, Bangladesh

Michael S. Steckler[1], Carol A. Wilson[2], Md. Hasnat Jaman[3], Steven L. Goodbred[4], Bar Oryan[5], Céline Grall[1], Scott DeWolf[7], Scott L. Nooner[8], S. Humayun Akhter[9]

1 Lamont -Doherty Earth Observatory of Columbia University, Palisades, NY, United States
2 Department of Geology and Geophysics, Louisiana State University, Baton Rouge, LA, United States
3Department of Geology and Mining, University of Barishal, Barishal, Bangladesh
4 Department of Earth and Environmental Sciences, Vanderbilt University, Nashville, TN, United States
5 Laboratoire de Géologie, Ecole Normale Supérieure, Paris, France.
6 LIENSs, La Rochelle University, La Rochelle, France
7 Department of Environmental Engineering and Earth Sciences, Clemson University, Clemson, SC, United States
8 Department of Earth and Ocean Sciences, University of North Carolina Wilmington, Wilmington, NC, United States
9 Vice Chancellor, Bangladesh Open University, Gazipur, Bangladesh
Contact: steckler@ldeo.columbia.edu

Introduction

Coastal regions worldwide face an ever-increasing sustainability issue as millions continue to migrate to these vulnerable regions susceptible to rising seas, increasing storms, and decimation of ecologically fragile areas. Deltas, the low-lying land at rivers mouths, are particularly sensitive to the delicate balance between sea level rise, land subsidence and sedimentation (e.g., Giosan et al., 2014). Bangladesh and the Ganges-Brahmaputra Delta (GBD) have been highlighted as a region at risk from sea level rise, but reliable estimates of land subsidence have been limited. While early studies in the GBD suggested high rates of relative sea level rise, recent papers estimate more modest rates. However, these estimates represent an aggregate of multiple, spatiotemporally variable processes that are not often separated into their relevant components. Furthermore, values for subsidence are typically taken as mean rates of vertical change and applied across entire delta systems, even where significant variations are well recognized (Passalacqua et al., 2021). Our objective is to better quantify the magnitude and spatial variability of subsidence in the GBD, to better evaluate the processes controlling it and the pattern of relative sea level rise in this vulnerable region.

Methods

To better understand subsidence, we use multiple measurements at different timescales and vertical sensitivity across the coastal zone of SW Bangladesh. At the longest timescales, Grall et al. (2018) used hand-drilled tube wells and a very high resolution seismic line to determine the Holocene-average subsidence rate. Several studies have used 300-600 year old Mosques, Hindu Temples and salt-making kilns to estimate centennial scale subsidence rates (Sarker et al., 2012; Hanebuth et al., 2013, 2021; Chamberlain et al., 2020; Steckler et al., 2022). Becker et al. (2020) analyzed tide and river gauges for decadal scale subsidence rates. We have rehabilitated older GNSS and installed new ones co-located with Rod Surface Elevation Tables-Marker Horizons (RSET-MH) to quantify the balance of subsidence and sedimentation in the coastal zone. The continuous GNSS installed in 2003 and 2012 were mounted on reinforced concrete building roofs. We also utilized a compaction meter array consisting of a set of 6 wells with depths from 20-300 m outfitted with optical fiber strainmeters (referred to as KHLC – the Khulna compaction meter; Steckler et al., 2022; DeWolf et al., in prep.).

Finally, in early 2020 we performed a campaign GNSS survey of 48 concrete Survey of Bangladesh (SoB) geodetic monuments in SW Bangladesh that were installed in 2002. Although only measured at the start and end of the period, the time span between the two measurements is ~18 years enabling us to estimate subsidence over this timespan. Sites were generally occupied for ~24 hrs, although some were established for up to 4 days.

Results

On longer timescales, Grall et al. (2018) find that Holocene averaged subsidence rates increase from the Hinge Zone of the early Cretaceous passive margin seaward (0 – 4.5 mm/yr). The rates from the 300-600 year old archeological sites are 1 – 4 mm/yr, similar to the estimated Holocene rates (Fig. 1; Sarker et al., 2012; Hanebuth et al., 2013, 2021; Chamberlain et al., 2020; Steckler et al., 2022).

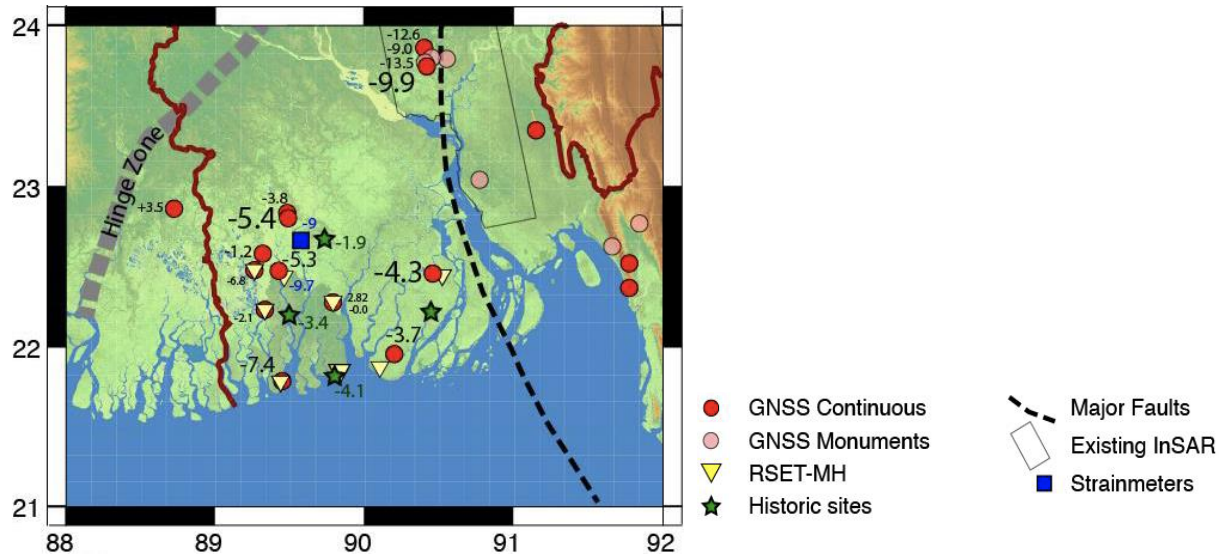

Figure 1 Subsidence rates in coastal GBD west of the deformation front (dashed line). Text size is proportional to the √(time series length) to represent the reliability of the values, except for historic sites. Historic sites values are similar to Holocene average rates in Grall et al. (2018) as are the rates at the easternmost GNSS sites. GNSS farther west rates are slightly higher, especially in the muddy Sundarbans Mangrove Forest. Rapid subsidence is seen in Dhaka, to the north due to groundwater withdrawal.

Decadal measurements from continuous GNSS stations and the tide gauges yield slightly higher subsidence rates of 3-7 mm/y (Fig. 1; Becker et al., 2020; Steckler et al., 2022). We note that while the tide gauges and GNSS rates are similar, the pattern of subsidence differs slightly. The more recent RSET-MH and vertical strainmeters (KHLC) show much higher rates of 9-10 mm/yr (Fig. 1; Bomer et al., 2019; Steckler et al., 2022). These instruments, in sites of active sedimentation, include a new spatial component: shallow subsidence that is not recorded by the deeply rooted river gauges and GNSS. However, it should be noted that continuous GNSS do include deep subsidence, which is not included by the RSET-MH or KHLC. These results combined indicate that there is a considerable amount of ongoing shallow sediment compaction.

Figure 2 shows newly obtained subsidence rates from the campaign GNSS sites. About half the sites yielded very high subsidence rates. We strongly suspect that the monuments at these sites are unstable and have undergone local (shallow) subsidence. To examine the possibility that the very high rates of subsidence recorded are due to monument instability, we reoccupied 4 sites near Barisal in October 2022 during a lull in COVID. Two sites with lower rates yielded linear trends for the three measurements. In contrast, the remaining two sites with higher subsidence rates yielded non-linear

subsidence. Thus, we exclude stations with these high rates from further analysis. The remaining sites show an increase in subsidence from the NW to the SE, consistent with estimates of average Holocene subsidence (Grall et al., 2018). However, rates from the campaign stations are still much higher than those from continuous GPS sites. We believe that the continuous building GPS omits very shallow compaction-related subsidence. The remaining 22 sites show an increase in subsidence from the NW to the SE (Fig. 2) consistent the pattern of Holocene subsidence (Grall et al., 2018). However, the rates increase from near zero in the NW to ~14-15 mm/y. The sites in the northwest that show little to no subsidence are where the Holocene sediments are sandy based on tube well drillings, while the remaining coastal sites are dominantly muddy (Fig. 2, bottom right). We note rates from the campaign GNSS are still much higher than those from continuous GNSS sites. We believe that the continuous GNSS buildings omit very shallow compaction-related subsidence.

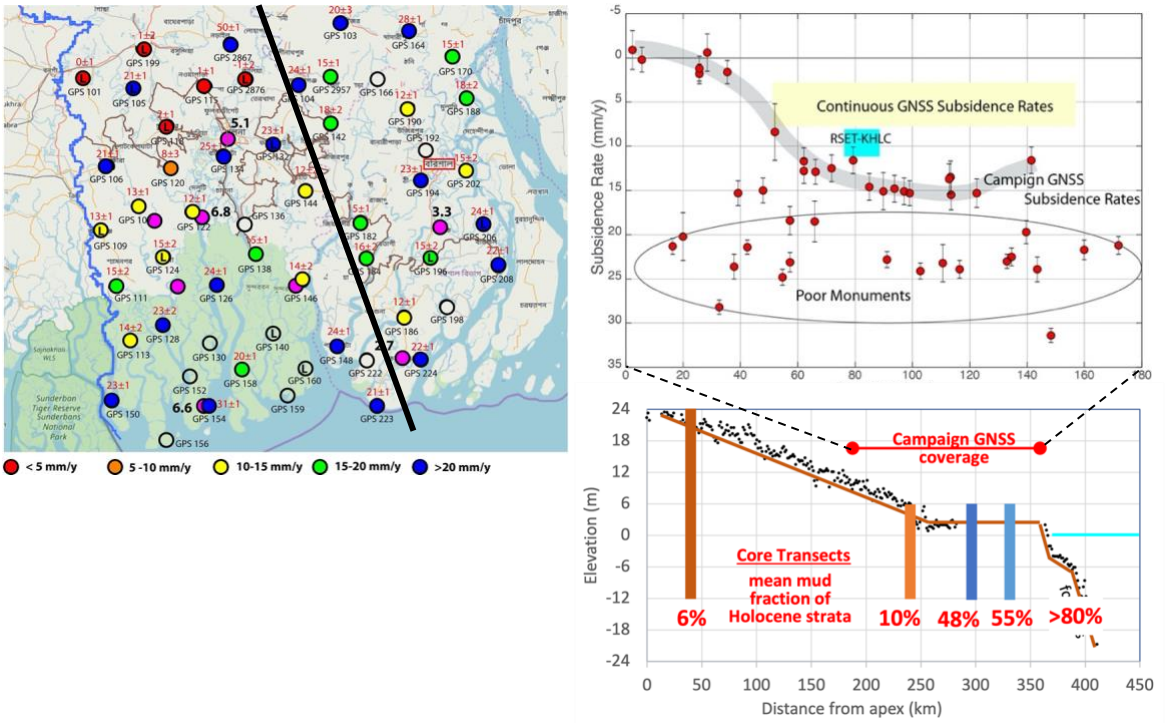

Figure 2 (Left) Position of the 55 geodetic monuments installed by the SoB in SW Bangladesh. We successfully remeasured 47 sites with campaign GNSS. Color-coded dots display the site names and average subsidence rates over ~18 years from 2002 to 2020. An 'L' indicates where leveling was used to link the GNSS to the monument because of poor sky view. Magenta dots are the positions of our continuous GNSS sites with their subsidence rates in bold black (Right) Transect of subsidence rates measured by campaign GNSS along the profile. The gray band shows the average subsidence rates from reliable measurements. We interpret the highest rates as unreliable due to settling or instability of the monuments, confirmed by selected reoccupation of 4 monuments in October 2020. (Lower Right) Plot showing the elevation and lithology change along the profile.

Conclusion

Steckler et al. (2022) found subsidence measurements using different methodologies exhibit variations that show systematic patterns spatially—both in the horizontal and with depth—and temporally (Fig. 3). Overall, subsidence rates are inversely time-dependent, with younger deposits consolidating at greater rates commensurate with their age (i.e., Sadler effect). GNSS subsidence rates near the Lower Meghna River are within about a millimeter/year of the Holocene rates. However, farther west, continuous GNSS subsidence rates are consistently a few mm/y higher than the longer-term rates (for example, the Sundarbans at 7.4 mm/y). We ascribe this difference to greater sediment compaction in the muddier sediments. Very high rates of subsidence are located north of the coastal zone near Dhaka (Fig. 1) due to groundwater extraction. Devices measuring shallow subsidence, the

RSET-MH and KHLC strainmeter, show higher rates of 9-10 mm/y (Fig. 1). These instruments, located in sites of active sedimentation, include shallow subsidence not recorded by either the river gauges or continuous GNSS. These GNSS sites are installed on reinforced concrete buildings which have foundations or footings below ground level. Continuous GNSS do include deep subsidence that occurs below the base of the RSET or strainmeters. The total subsidence at a site with active sedimentation may be equal to the values obtained by the campaign GNSS and may therefore reach values of 14-15 mm/y. Parsing the subsidence rates by depth, we estimate that the deep subsidence from below the Holocene strata is 2-3 mm/y and likely due to isostatic loading (Fig. 3). There is little contribution from sediment compaction at great depths due to the deep incision of the river valleys during the last ice age. Deeper sediments will not start to compact again until the weight of the sediments above them exceed the maximum reached before the incision. At intermediate depths (Fig. 3), perhaps corresponding to the Holocene, we estimate only 1-4 mm/y.

There appears to be a lithologic control north to south (Fig. 2), and in the coastal zone east to west (Fig. 1), whereby sandier sediments impart lower compaction and subsidence in the GBD. Continuous GNSS subsidence rates are consistently a few mm/y higher towards the SW, farther from the sandy main mouth of the Ganges River. Similarly, there is minimal subsidence of the 5 campaign sites to the NW (red circles; Fig. 2). At these sites, Holocene sediments are only ~10% mud, much lower than farther south where they are 48-80% mud.

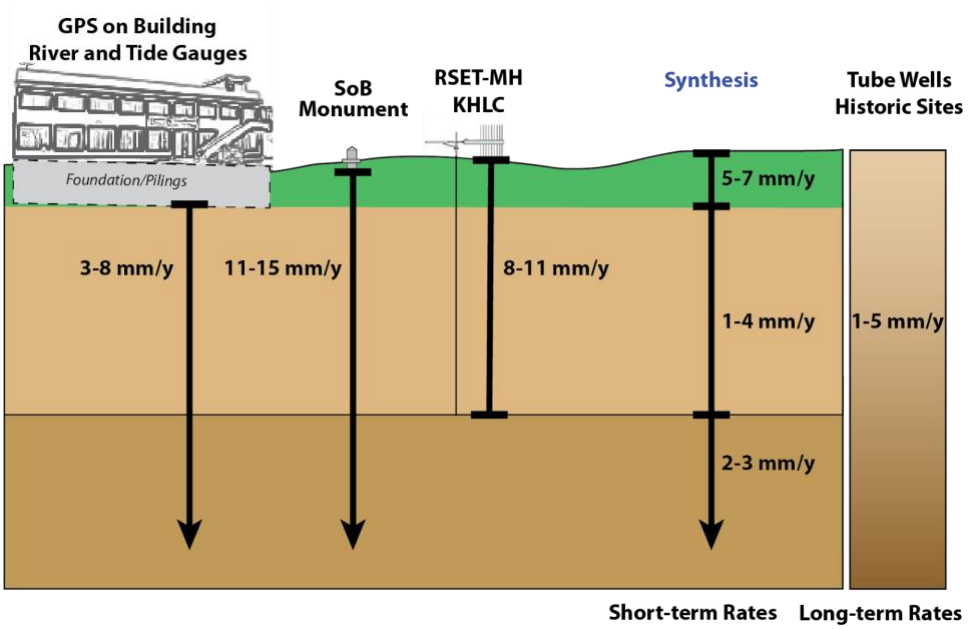

Figure 3 Cartoon presenting a synthesis of subsidence versus depth based on combining measurements from multiple instruments, each of which measure compaction or subsidence over a different depth range. GNSS on building and tide gauges measure subsidence below the building or gauge foundations and miss shallow compaction. The RSET-MH and KHLC measure compaction above the base of their instruments. The campaign GNSS on SoB monuments measures both shallow and deep subsidence. Combining the results, the synthesis column shows a preliminary estimate of subsidence in each depth range. The long-term rates correspond to the sum of the two deeper brown layers.

References

Bahr, D.B., Hutton, E.W.H., Syvitski, J.P.M., Pratson, L.F., (2001). Exponential approximations to compacted sediment porosity profiles. Computers & Geosciences 27, 691–700.

Becker, M., F. Papa, M. Karpytchev, C. Delebecque, Y. Krien, J.U. Khan, V. Ballu, F. Durand, G. Le Cozannet, A.K.M.S. Islam, S. Calmant, C.K. Shum (2020). Water level changes, subsidence, and sea level rise in the Ganges–Brahmaputra–Meghna delta, Proceedings of the National Academy of Sciences, 117 (4) 1867-1876; doi:10.1073/pnas.1912921117.

Bomer, E.J., C.A. Wilson and D.K. Datta, (2019). An Integrated Approach for Constraining Depositional Zones in a Tide-Influenced River: Insights from the Gorai River, Southwest Bangladesh, Water 11, 2047; doi:10.3390/w11102047

Chamberlain, E.L., S.L. Goodbred, R. Hale, M.S. Steckler, J. Wallinga, C. Wilson (2020). Integrating geochronologic and instrumental approaches across the Bengal Basin, Earth Surface Processes and Landforms, 45, 56-74., https://doi.org/10.1002/esp.4687.

Giosan, L, J. Syvitski, S. Constantinescu and J. Day (2014). Protect the world's deltas. Nature 516, 31–33.

Grall, C., M.S. Steckler, J.L. Pickering, S. Goodbred, R. Sincavage, C. Paola, S.H Akhter, V. Spiess (2018). A base-level stratigraphic approach to determining Holocene subsidence of the Ganges–Meghna–Brahmaputra Delta plain. Earth and Planetary Science Letters, Earth and Planetary Science Letters 499, 23–36, 10.1016/j.epsl.2018.07.008.

Hanebuth, T.J.J., Kudrass, H.R., Linstaedter, J., Islam, B., Zander, A.M., (2013). Rapid coastal subsidence in the central Ganges–Brahmaputra Delta (Bangladesh) since the 17th century deduced from submerged salt-producing kilns. Geology 41 (9), 987–990. http://dx.doi.org/10.1130/G34646.1.

Hanebuth, T.J.J., Kudrass, H.R., Zander, A.M., Akhter, H.S., Neumann-Denzau, G., Zahid, A., (2021). Stepwise, earthquake-driven coastal subsidence in the Ganges–Brahmaputra Delta (Sundarbans) since the eighth century deduced from submerged in situ kiln and mangrove remnants. Nat. Hazards.

Passalacqua, P., Goodbred, S., Giosan, L., Overeem, I., (2021). Stable ≠ Sustainable: Delta dynamics versus the human need for stability, Earth's Future. 10.1029/2021EF002121

Sarker, M.H., Choudhury, G.A., Akter, J., Hore, S.K., (2012). Bengal Delta Not Sinking at a Very High Rate. Daily Star (23rd December 2012).

Steckler, M.S., B. Oryan, C.A. Wilson, C. Grall, S.L. Nooner, D.R. Mondal, S.H. Akhter, S. DeWolf, S.L. Goodbred, Synthesis of the Distribution of Subsidence of the Lower Ganges-Brahmaputra Delta, Bangladesh, Earth-Science Reviews, 224, 103887, doi:10.1016/j.earscirev.2021.103887.